

Broadband pseudo-thermal states with tunable spectral coherence generated via nonlinear optics

Nicolás Quesada and Agata M. Brańczyk*

Perimeter Institute for Theoretical Physics, Waterloo, Ontario, N2L 2Y5, Canada

It is well known that the reduced state of a two-mode squeezed vacuum state is a thermal state—i.e. a state whose photon-number statistics obey a geometric distribution. More exotic *broadband* states can be realized as the reduced state of two spectrally-entangled beams generated using nonlinear optics. We show that these broadband “pseudo-thermal” states are tensor products of states in spectral Schmidt modes, whose photon-number statistics obey a geometric distribution. We study the spectral and temporal coherence properties of these states and show that their spectral coherence can be tuned—from perfect coherence to complete incoherence—by adjusting the pump spectral width. In the limit of a CW pump, these states are tensor products of true thermal states, but with different temperatures at each frequency. This could be an interesting state of light for investigating the interplay between spectral, temporal, and photon-number coherences.

I. INTRODUCTION

Thermal states are of fundamental and practical interest. Although they are diagonal in the photon-number and coherent-state bases, they can behave non-classically. They can be used for generating non-classical states [1, 2], or for mediating entanglement between quantum systems [3]. They can also be used for quantum information protocols such as continuous-variable quantum key distribution [4], and improving the efficiency of quantum state tomography [5].

In quantum information, one often deals with single-mode thermal states. There, the relevant property is the photon-number statistics—the thermal state density matrix is diagonal with a geometric probability distribution.

In quantum optics, when considering many radiation modes, the temperature T takes a more central role as it determines the light’s spectral radiance according to Planck’s law. For multimode thermal light, one can speak about its spatial, spectral, temporal, and momentum coherence.

Incoherence in these degrees of freedom can be useful. Spatially incoherent light has been used for ghost imaging [6–12], sub-wavelength lithography [13], and improving diffraction pattern visibility [14] and spatial resolution [15]. Broadband spectrally incoherent light has been used for resolution-enhanced optical coherence tomography [16], optical guiding of microscopic particles [17], and noisy-light spectroscopy [18, 19].

Various methods exist for generating incoherent

light. Spatially incoherent, pseudo-thermal light can be generated by sending a CW laser through a rotating ground-glass disc [20–22]. Broadband, spectrally incoherent light can be generated by a thermal source—e.g. a hollow cathode lamp [9]. Other approaches use amplified spontaneous emission from quantum dots, [23, 24], warm atomic vapour [25], and modified dye lasers [26]. Here, we focus on light generated in one arm of a broadband twin-beam state, such as that generated via spontaneous parametric downconversion (SPDC) [27, 28] or spontaneous four wave mixing (SFWM) [29]. Spectral entanglement between the beams makes each individual beam spectrally incoherent.

Photon statistics and coherence can be studied by measuring correlation functions. Various groups measured such functions on light generated via nonlinear optics. These include measurements of time-resolved temporal correlation functions in CW-pumped SPDC [30], time-averaged temporal correlation functions in two-mode SPDC [27, 31], frequency cross- and auto-correlation functions in two-mode SPDC [32], multi-photon statistics of single-mode SPDC [33], and frequency-resolved spectral correlation functions and multi-photon statistics in harmonic generation [28]. Theory has also been done on photon-number statistics [34] and spatial correlation functions [6, 7] of downconverted light.

But to the best of our knowledge, no one has written down the reduced density operator for one arm of an arbitrary spectrally-entangled twin-beam state. Nor has anyone computed its time-resolved temporal and frequency-resolved spectral correlation functions.

In this paper, we show that the density operator describing one arm of a twin-beam state with arbitrary spectral entanglement can be decomposed

*Electronic address: abranczyk@pitp.ca

into a tensor product of states prepared in spectral Schmidt modes, each with geometric photon-number statistics. We therefore refer to the state as a broadband “pseudo-thermal” (BPT) state.

We then write down Heisenberg-picture operators for the Schmidt modes and compute the BPT state’s frequency-resolved spectral and time-resolved first- and second-order correlation functions. These functions reveal the light’s spectral and temporal coherence, as well as its intensity-intensity correlations. We find that the spectral coherence of BPT states can be tuned—from perfect coherence to full incoherence—by adjusting the pump spectral width. This is consistent with recent experiments [31]. The spectral coherence can also be tuned by changing the spectral phase of the pump, e.g. by applying a chirp [35], although we do not consider this here.

From these correlation functions, once can identify interesting regimes not yet explored experimentally, such as partial spectral coherence. The shape of these functions also make clear the connection between our BPT state and the partially-coherent pseudo-thermal states recently generated by warm atomic vapor [25] and intensity modulated laser light sent through rotating ground glass [36].

While the density operator for the BPT state was derived from a twin-beam state, the expression can be used to model pseudo-thermal light created with completely different methods, e.g., [24–26, 36]. This is because any mixed state can be realized as a pure state in a larger Hilbert space [37]. Given a density operator for partially-coherent light, one can compute any correlation function or other quantity of interest.

Our results should therefore be useful for both experimental and theoretical studies of partially-spectrally-coherent light.

II. BROADBAND TWO-MODE SQUEEZED VACUUM STATE

We consider broadband light, generated by e.g. SPDC or SFWM, emitted into two orthogonal modes. In a one dimensional propagation geometry where the longitudinal wave vector is specified by the frequency, and assuming that the pump beam remains un-depleted, the twin-beam state is:

$$|\psi\rangle = \hat{U}_{\text{SQ}} |\text{vac}\rangle ; \quad (1)$$

$$\hat{U}_{\text{SQ}} = e^{(\iint d\omega_a d\omega_b J(\omega_a, \omega_b) \hat{a}^\dagger(\omega_a) \hat{b}^\dagger(\omega_b) - \text{H.c.})}, \quad (2)$$

where $J(\omega_a, \omega_b)$ is known as the *joint spectral amplitude* (JSA) of the generated beams [38–40] and \hat{U}_{SQ}

is the broadband two-mode squeezing operator. The operators $\hat{a}(\omega)$ and $\hat{b}(\omega)$ are single-frequency annihilation operators that satisfy the commutation relations $[\hat{a}(\omega), \hat{a}^\dagger(\omega')] = [\hat{b}(\omega), \hat{b}^\dagger(\omega')] = \delta(\omega - \omega')$ (all other commutators are zero). The JSA depends on the properties of the pump field(s) and the nonlinear material. For purposes of this paper, we leave it quite general.

To simplify calculations, the JSA can be decomposed as $J(\omega_a, \omega_b) = \sum_k r_k \phi_k(\omega_a) \varphi_k(\omega_b)$, in what is known as the Schmidt decomposition [41]. The twin-beam state can then be written as [27]:

$$|\psi\rangle = e^{\sum_k r_k \hat{A}_k^\dagger \hat{B}_k^\dagger - \text{H.c.}} |\text{vac}\rangle, \quad (3)$$

where the operators

$$\hat{A}_k = \int d\omega_a \phi_k^*(\omega_a) \hat{a}(\omega_a), \quad (4a)$$

$$\hat{B}_k = \int d\omega_b \varphi_k^*(\omega_b) \hat{b}(\omega_b), \quad (4b)$$

are broadband annihilation operators that satisfy the commutation relations $[\hat{A}_k, \hat{A}_{k'}^\dagger] = [\hat{B}_k, \hat{B}_{k'}^\dagger] = \delta_{k,k'}$ (all other commutators are zero), and ϕ_k and φ_k are known as Schmidt modes; these functions satisfy completeness and orthogonality relations (cf. [42]). One can also invert the relations in Eqs. (4) and find

$$\hat{a}(\omega) = \sum_k \phi_k(\omega) \hat{A}_k, \quad (5a)$$

$$\hat{b}(\omega) = \sum_k \varphi_k(\omega) \hat{B}_k. \quad (5b)$$

The twin-beam state in Eq. (3) can be rewritten as:

$$|\psi\rangle = \bigotimes_k |r_k\rangle, \quad (6)$$

where

$$|r_k\rangle = e^{r_k \hat{A}_k^\dagger \hat{B}_k^\dagger - \text{H.c.}} |\text{vac}\rangle \quad (7)$$

is a two-mode squeezed vacuum (TMSV) state prepared in two Schmidt modes ϕ_k and φ_k , with *squeezing parameter* $r_k \geq 0$. Note that here $J(\omega_a, \omega_b)$ is not necessarily normalized and thus $\sum_k r_k^2$ does not necessarily equal 1. Each TMSV state can be represented in the number basis

$$|r_k\rangle = \sum_{n_k=0}^{\infty} \frac{(\tanh r_k)^{n_k}}{\cosh(r_k)} |n_k\rangle_{\phi_k} |n_k\rangle_{\varphi_k}. \quad (8)$$

In the Heisenberg picture, the operators \hat{A}_k and \hat{B}_k transform as:

$$\begin{aligned}\hat{A}_k &\rightarrow \hat{\mathcal{U}}_{\text{SQ}}^\dagger \hat{A}_k \hat{\mathcal{U}}_{\text{SQ}} \\ &= \cosh(r_k) \hat{A}_k + \sinh(r_k) \hat{B}_k^\dagger,\end{aligned}\quad (9a)$$

$$\begin{aligned}\hat{B}_k &\rightarrow \hat{\mathcal{U}}_{\text{SQ}}^\dagger \hat{B}_k \hat{\mathcal{U}}_{\text{SQ}} \\ &= \cosh(r_k) \hat{B}_k + \sinh(r_k) \hat{A}_k^\dagger.\end{aligned}\quad (9b)$$

Later, we will use the relations in Eqs. (5) and the transformation in Eqs. (9) to compute correlation functions.

III. BROADBAND THERMAL-LIKE STATES

We are interested in the quantum state of the individual beams, we thus compute the reduced density matrices for modes a and b by tracing out the other mode. The density operator for mode a is

$$\rho_a = \text{Tr}_b[|\psi\rangle\langle\psi|] = \bigotimes_k \rho_{\phi_k}, \quad (10)$$

where

$$\rho_{\phi_k} = \text{Tr}_{\varphi_k}[|r_k\rangle\langle r_k|] \quad (11)$$

$$= \sum_{n_k=0}^{\infty} P_{n_k} |n_k\rangle_{\phi_k} \langle n_k|_{\phi_k}, \quad (12)$$

is a state prepared in a single Schmidt mode ϕ_k . The states $|n_k\rangle_{\phi_k} = (n_k!)^{-1/2} (\hat{A}_k^\dagger)^{n_k} |0\rangle$ are broadband Fock states, and are distributed according to

$$P_{n_k} = \frac{1}{1 + \bar{n}_k} \left(\frac{\bar{n}_k}{1 + \bar{n}_k} \right)^{n_k}, \quad (13)$$

where

$$\bar{n}_k = \sinh^2(r_k). \quad (14)$$

The state ρ_{ϕ_k} is like a single-mode thermal state in the sense that it is diagonal in the photon-number basis and the probability distribution is geometric. But since the mode is not at a well-defined frequency, it doesn't make sense to talk about an associated temperature T .

Similarly, the beam in mode b has the state $\rho_b = \bigotimes_k \rho_{\varphi_k}$ where $\rho_{\varphi_k} = \sum_{n_k=0}^{\infty} P_{n_k} |n_k\rangle_{\varphi_k} \langle n_k|_{\varphi_k}$. While both ρ_a and ρ_b obey the same statistics given by P_{n_k} , the states will have different spectral and temporal properties because the spectral properties of $|n_k\rangle_{\phi_k}$ differ from those of $|n_k\rangle_{\varphi_k}$.

The states in Eq. (12) can be written more succinctly as

$$\rho_{\phi_k} = \frac{1}{Z_k} e^{-\alpha_k \hat{A}_k^\dagger \hat{A}_k}; \quad (15)$$

$$Z_k = \text{Tr} \left(e^{-\alpha_k \hat{A}_k^\dagger \hat{A}_k} \right) = \frac{1}{1 - e^{-\alpha_k}}, \quad (16)$$

where Z_k is the partition function of mode k and

$$e^{-\alpha_k} = \tanh^2(r_k) = \frac{\bar{n}_k}{1 + \bar{n}_k}. \quad (17)$$

Using this notation we can also write the full state in mode a as

$$\rho_a = \frac{1}{Z} e^{-\sum_k \alpha_k \hat{A}_k^\dagger \hat{A}_k}; \quad (18)$$

$$Z = \text{Tr} \left(e^{-\sum_k \alpha_k \hat{A}_k^\dagger \hat{A}_k} \right). \quad (19)$$

IV. PROPERTIES OF BROADBAND THERMAL-LIKE STATES

To study the coherence properties of the broadband states, we compute various temporal and spectral correlation functions. The expressions for mode a can be mapped to those for mode b by making the substitution: $\phi_k \rightarrow \varphi_k$.

A. Spectral correlation function

To study the spectral coherence properties of the light, we introduce a spectral correlation function $S(\omega, \omega')$. Using the procedure outlined in Appendix A, one finds that

$$S_a(\omega, \omega') = \langle \hat{a}^\dagger(\omega) \hat{a}(\omega') \rangle_\psi \quad (20)$$

$$= \sum_k \sinh^2(r_k) \phi_k^*(\omega) \phi_k(\omega'), \quad (21)$$

and also that $\langle \hat{a}(\omega) \hat{a}(\omega') \rangle_\psi = \langle \hat{a}^\dagger(\omega) \hat{a}^\dagger(\omega') \rangle_\psi = 0$.

The same-frequency correlation function is

$$S_a(\omega, \omega) = \sum_k |\phi_k(\omega)|^2 \bar{n}_k, \quad (22)$$

which can be interpreted as the spectral density of the light.

B. First-order temporal correlation function

The first-order temporal correlation function for mode a is [43]:

$$G_a^{(1)}(t_1, t_2) = \langle \hat{a}^\dagger(t_1) \hat{a}(t_2) \rangle_\psi, \quad (23)$$

in the limit of the state $|\psi\rangle$ having sufficiently narrow frequency support this quantity is proportional to $\langle \hat{E}^{(-)}(t_1) \hat{E}^{(+)}(t_2) \rangle_\psi$ where $\hat{E}_a^{(\pm)}(t_1)$ are the usual positive/negative frequency components of the electric field operator in mode a . The operators $\hat{a}(t)$ are nothing but the Fourier transform of the operators $\hat{a}(\omega)$

$$\hat{a}(t) = \frac{1}{\sqrt{2\pi}} \int d\omega \hat{a}(\omega) e^{i\omega t}. \quad (24)$$

We thus have

$$G_a^{(1)}(t_1, t_2) = \langle \hat{a}^\dagger(t_1) \hat{a}(t_2) \rangle_\psi \quad (25)$$

$$= \int \frac{d\omega d\omega'}{2\pi} S(\omega, \omega') e^{-i\omega t_1 + i\omega' t_2} \quad (26)$$

$$= \sum_k \tilde{\phi}_k^*(t_1) \tilde{\phi}_k(t_2) \bar{n}_k, \quad (27)$$

where \bar{n}_k is defined in Eq. (14), and where

$$\tilde{\phi}_k(t) = \frac{1}{\sqrt{2\pi}} \int d\omega \phi_k(\omega) e^{i\omega t}. \quad (28)$$

This expression is derived in Appendix B. To see the temporal distribution, we compute

$$G_a^{(1)}(t, t) = \sum_k |\tilde{\phi}_k(t)|^2 \bar{n}_k, \quad (29)$$

which can be interpreted as the probability per unit time that a photon is absorbed by an ideal detector at time t [43].

C. Second-order temporal correlation function

To see intensity-intensity correlations, we look at the second-order correlation function [43]:

$$G^{(2)}(t_1, t_2) = \langle \hat{a}^\dagger(t_1) \hat{a}^\dagger(t_2) \hat{a}(t_1) \hat{a}(t_2) \rangle_\psi \quad (30)$$

$$= G_a^{(1)}(t_1, t_1) G_a^{(1)}(t_2, t_2) + G_a^{(1)}(t_1, t_2) G_a^{(1)}(t_2, t_1), \quad (31)$$

where we again replaced the electric field operators with photon number creation and destruction operators, and where $G_a^{(1)}(t_1, t_2)$ is defined in Eq. (26).

This expression is derived in Appendix B. Eq. (31) can be interpreted as the probability per unit (time)² that one photon is recorded at time t_1 and another at time t_2 [43].

V. CONTINUOUS WAVE LIMIT

In the case of a CW laser driving an SPDC process at frequency $\bar{\omega}_p$ (or a SFWM process at $\bar{\omega}_p/2$), energy is conserved according to $\omega_a + \omega_b = \bar{\omega}_p$. The two-mode squeezed state has the form

$$|\psi\rangle = \hat{\mathcal{U}}_{\text{SQ}} |\text{vac}\rangle; \quad (32)$$

$$\hat{\mathcal{U}}_{\text{SQ}} = e(\int d\omega r(\omega) \hat{a}^\dagger(\omega) \hat{b}^\dagger(\bar{\omega}_p - \omega) - \text{H.c.}), \quad (33)$$

We can also construct Heisenberg picture transformation (similar to the pulsed-pump case):

$$\hat{a}(\omega) \rightarrow \hat{\mathcal{U}}_{\text{SQ}}^\dagger \hat{a}(\omega) \hat{\mathcal{U}}_{\text{SQ}} \quad (34)$$

$$= \cosh(r(\omega)) \hat{a}(\omega) + \sinh(r(\omega)) \hat{b}^\dagger(\omega_p - \omega) \quad (35)$$

$$\hat{b}(\omega) \rightarrow \hat{\mathcal{U}}_{\text{SQ}}^\dagger \hat{b}(\omega) \hat{\mathcal{U}}_{\text{SQ}} \quad (36)$$

$$= \cosh(r(\omega)) \hat{b}(\omega) + \sinh(r(\omega)) \hat{a}^\dagger(\omega_p - \omega), \quad (37)$$

and also write states for mode a (or b)

$$\rho_a = \frac{1}{Z} e^{-\int d\omega \alpha(\omega) \hat{a}^\dagger(\omega) \hat{a}(\omega)}, \quad (38)$$

$$Z = \text{Tr} \left(e^{-\int d\omega \alpha(\omega) \hat{a}^\dagger(\omega) \hat{a}(\omega)} \right), \quad (39)$$

where $\alpha(\omega) = \log(1/\tanh^2(r(\omega)))$. By generalizing the result in Appendix A, from a discrete to a continuum index, the spectral correlation function becomes

$$S_{\text{CW}}(\omega, \omega') = \bar{n}_{\text{CW}}(\omega) \delta(\omega - \omega'), \quad (40)$$

$$\bar{n}_{\text{CW}}(\omega) = \sinh^2(r(\omega)). \quad (41)$$

Eq. (40) tells us that there are no spectral correlations between two different frequency modes.

If one sets $\alpha(\omega) = \hbar\omega/k_B T$, then ρ_a can be thought of as a multi-mode thermal state in the traditional sense. The shape of $\alpha(\omega)$ depends on $r(\omega)$ which in turn depends on the nonlinearity profile of the material. It would therefore be difficult to make light that exactly matches the Planck spectrum. But one could match the Planck spectrum over a finite bandwidth, or make more general states where each frequency corresponds to a thermal state at a different temperature T .

The first-order correlation function for CW broadband thermal light is the two-dimensional Fourier

transform of $S_{\text{CW}}(\omega, \omega')$. After integrating out the Dirac delta function, this becomes

$$G_{\text{CW}}^{(1)}(t_1, t_2) = \frac{1}{2\pi} \int d\omega e^{i\omega(t_1 - t_2)} \bar{n}_{\text{CW}}(\omega), \quad (42)$$

as expected from the Wiener-Khinchin theorem. From this, we can compute:

$$G_{\text{CW}}^{(1)}(t, t) = \frac{1}{2\pi} \int d\omega \bar{n}_{\text{CW}}(\omega). \quad (43)$$

That Eq. (43) is constant also shows that the light is fully spectrally incoherent, since time-varying intensities arise from well-defined phases between frequencies. Similarly, the second-order correlation function for CW-pumped BPT states is

$$G_{\text{CW}}^{(2)}(t_1, t_2) = G_{\text{CW}}^{(1)}(t_1, t_1) G_{\text{CW}}^{(1)}(t_2, t_2) + G_{\text{CW}}^{(1)}(t_1, t_2) G_{\text{CW}}^{(1)}(t_2, t_1), \quad (44)$$

where $G_{\text{CW}}^{(1)}(t_1, t_2)$ is defined in Eq. (42). If one sets $\alpha(\omega) = \hbar\omega/k_B T$, Eq. (44) is identical to the expression for $G^{(2)}(t_1, t_2)$ for chaotic light, derived by, e.g., Loudon [44].

VI. EXAMPLES

To illustrate the pump laser's impact on the coherence of BPT states, we examine the concrete case of SPDC. We look at three examples: short pulse; long pulse; and CW.

For simplicity, we consider pump fields with Gaussian spectral distributions (e.g., shaped using optical pulse-shaping [45]), and crystals with Gaussian nonlinearity profiles (e.g., engineered using nonlinearity shaping methods [46–50]). We consider the system to be in the low-gain regime and satisfy symmetric group-velocity-matching [51–53].

We take

$$J(\Omega_a, \Omega_b) = A e^{-\frac{(\Omega_a + \Omega_b)^2}{2\sigma_p^2}} e^{-\frac{(\Omega_a - \Omega_b)^2}{2\sigma_c^2}} \quad (45)$$

for the pulsed case, where $\Omega_j = \omega_j - \bar{\omega}_j$ (with $\bar{\omega}_j$ the mean frequency of the downconverted beam), σ_p is the spectral width of the pump amplitude function, and σ_c is the width of the phase-matching function (given as the Fourier transform of the longitudinal shape of the material nonlinearity). We also take

$$r(\Omega) = A e^{-\frac{(2\Omega)^2}{2\sigma_c^2}}, \quad (46)$$

pump	A	σ_p	σ_c
short	1.9×10^{-13} s	2×10^{12} s ⁻¹	2×10^{12} s ⁻¹
long	7.3×10^{-13} s	1×10^{11} s ⁻¹	3×10^{12} s ⁻¹
CW	3.1×10^{-7}	n/a	3×10^{12} s ⁻¹

TABLE I: Parameters used to generate Figure 1.

for the CW case, where $\Omega = \omega - \bar{\omega}_a$. For easy comparison, we chose A , σ_p and σ_c to make BPT states with similar spectral distributions (Table I). Figure 1 compares the three examples.

Figure 1 (a) shows the JSA of the twin-beam state. The JSA for the short-pulse case is separable (note that this only happens for a pair of *Gaussians* of the same width [54]). The long-pulsed laser leads to a correlated JSA, and the CW laser leads to a strongly correlated JSA.

Figure 1 (b) shows the spectral distributions of the BPT state in mode a . The spectra for all examples are almost the same.

Figure 1 (c) shows the temporal distributions of the BPT state in mode a . These vary drastically for all examples. Because the short pump yields a separable JSA, the BPT state is prepared in a single, broad, yet coherent, spectral mode. This means that the frequencies have fixed relative phases, which leads to a spectrally-coherent pulse of pseudo-thermal light. As the pump pulse-length grows, the pseudo-thermal pulse gets longer. In turn, the relative phases of the frequencies become less fixed. In the limit of a CW pump, the BPT state is also continuous, but broadband, and the frequencies have *no* fixed relative phase relationship.

Figure 1 (d) shows the normalized time-resolved first-order temporal correlation function for the BPT state in mode a . The light in all three examples has roughly the same coherence time, although the short-pulse case has a slightly shorter coherence time, despite having very similar spectra to the longer-pulse cases. We note that since a pulse is not stationary, it does not have to satisfy the Wiener-Khinchin theorem. Figure 1 (e) shows the normalized time-resolved second-order temporal correlation function for the BPT state in mode a . This function represents two broadband detection events at times separated by τ , at the same position. In all cases, two-photon absorptions is very likely for small τ . For longer pump fields, the probability of absorbing two photons is non-zero for larger τ . We note that in the short-pulse pump example, the pulse duration (c) and the intensity-intensity correlation time (e) are the same.

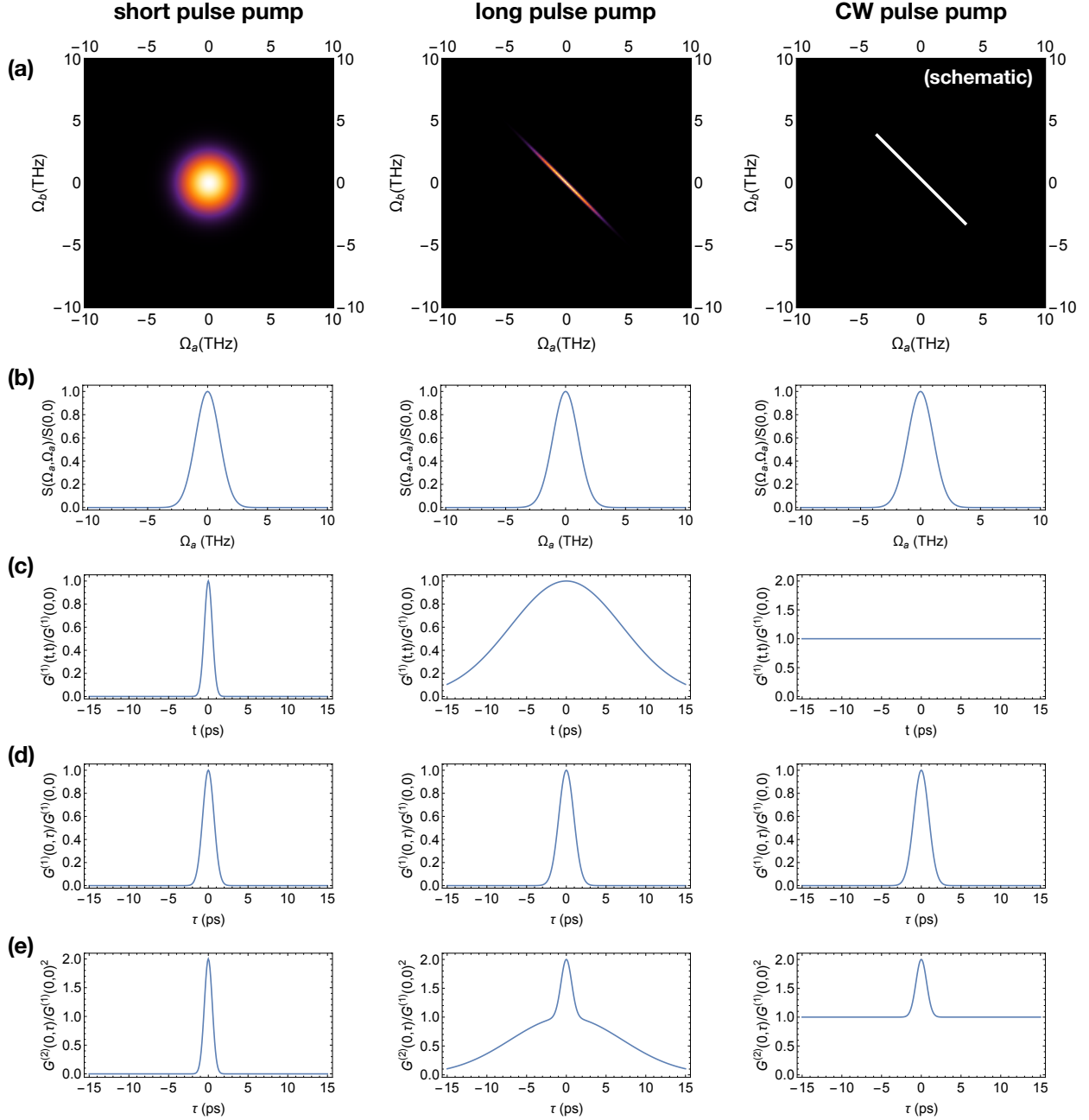


FIG. 1: Comparison between sources pumped by a short-pulsed, long-pulsed and CW laser: (a) the joint spectral amplitude $J(\omega_1, \omega_2)$; (b) equal-frequency spectral correlation function (normalized), (c) equal-time first-order temporal correlation function (normalized); (d) time-separated first-order temporal correlation function (normalized); and (e) time-separated second-order temporal correlation function (normalized). To see experimental data qualitatively similar to (e) for the long-pulse example, refer to, e.g., Fig 4. of [25] for measurements of broadband pseudo-thermal light generated from warm atomic vapor, or Fig. 8 of [36] for measurements of pseudo-thermal light generated with intensity modulated laser light passing through rotating ground glass.

In summary, these examples show that by varying the spectrum of the pump field as well as the shape of the nonlinearity function of the material, it is possible to generate various states of light with the same spectrum, very similar temporal coherence, and drastically different spectral coherence and two-photon absorption properties.

VII. DISCUSSION

Broadband thermal-like states generated via nonlinear optical processes, such as SPDC or SFWM, have interesting coherence properties. We calculated their spectral and temporal correlation functions in terms of the Schmidt modes of the joint spectral amplitude. We showed that these states have tuneable spectral coherence—which can be tuned from perfectly spectrally coherent to completely incoherent. Regardless of the level of spectral coherence, these states can be decomposed into tensor products of states with geometric photon-number statistics.

High-gain SPDC can be extremely bright for a parametric process—up to hundreds of mW mean power [28, 55, 56]. This is close to the ~ 1 W achievable via non-parametric processes [18], and is bright enough to study interesting non-classical phenomena such as the interplay between spectral and photon-number coherence. Furthermore, a source based on SPDC is extremely customizable. Beyond tuning the spectral coherence, the spectral shape can be customized using optical pulse-shaping [45] or nonlinearity shaping methods [46–50].

Broadband spectrally incoherent light generated by nonlinear optics may also have application in studying the dynamics of photoinduced processes, such as the time scales and mechanisms underlying the initial step of photosynthesis in light-harvesting complexes. Some researchers have questioned whether dynamics initiated by sunlight excitation might be different from those detected in femtosecond laser experiments performed on light-harvesting complexes [57–61]. A broadband source with tuneable spectral coherence might help answer this question.

On the theory side, this work is relevant to the study of decompositions of thermal light into broadband coherent modes. Thermal light cannot be represented as a statistical mixture of single pulses

[62], but one can construct mixtures of single pulses that yield the same first-order temporal correlation function as thermal light [63]. In a one-dimensional waveguide, thermal light was shown to decompose into a statistical mixture of sets of coherent pulses [64]. Here, we show that partially-spectrally-coherent light can be decomposed into a tensor product of states prepared in spectral Schmidt modes, each with geometric photon-number statistics. Our work also connects with decompositions, into Schmidt-like modes, of correlation functions for partially spatially coherent thermal light [65].

Our formalism also provides a convenient tool for computing any observables of broadband thermal-like states with partial spectral coherence—even for states created with completely different experimental methods, such as [23–26, 36]. This is due to a well-known result in quantum information theory, the Stinespring dilation theorem [37], that states that any mixed state can be represented as a pure state in a higher-dimensional Hilbert space. Any broadband thermal-like state can therefore be written as the reduced state of a hypothetical broadband twin-beam state.

The relationship between spectral, temporal, and photon-number coherence is of fundamental and practical interest. We hope that our analysis of broadband thermal-like states generated via nonlinear optics provides a useful way of exploring it theoretically and experimentally.

Acknowledgements

The authors thank John Sipe for helpful discussions, and John Donohue for helpful comments on the manuscript.

Funding Information

Research at Perimeter Institute is supported by the Government of Canada through Industry Canada and by the Province of Ontario through the Ministry of Research and Innovation. We acknowledge the support of the Natural Sciences and Engineering Research Council of Canada.

[1] A. Zavatta, V. Parigi, and M. Bellini, “Experimental nonclassicality of single-photon-added thermal

light states,” *Phys. Rev. A* **75**, 052106 (2007).

- [2] R. Tahira *et al.*, “Entanglement of Gaussian states using a beam splitter,” *Phys. Rev. A* **79**, 023816 (2009).
- [3] M. S. Kim, “Entanglers: Beam splitters and Thermal fields,” *Fortschritte der Physik* **50**, 652 (2002).
- [4] C. Weedbrook, S. Pirandola, and T. C. Ralph, “Continuous-variable quantum key distribution using thermal states,” *Phys. Rev. A* **86**, 022318 (2012).
- [5] G. Harder *et al.*, “Tomography by Noise,” *Phys. Rev. Lett.* **113**, 070403 (2014).
- [6] A. Gatti *et al.*, “Correlated imaging, quantum and classical,” *Phys. Rev. A* **70**, 013802 (2004).
- [7] A. Gatti *et al.*, “Ghost Imaging with Thermal Light: Comparing Entanglement and Classical Correlation,” *Phys. Rev. Lett.* **93**, 093602 (2004).
- [8] A. Valencia *et al.*, “Two-Photon Imaging with Thermal Light,” *Phys. Rev. Lett.* **94**, 063601 (2005).
- [9] D. Zhang *et al.*, “Correlated two-photon imaging with true thermal light,” *Opt. Lett.* **30**, 2354 (2005).
- [10] I. N. Agafonov *et al.*, “High-visibility intensity interference and ghost imaging with pseudo-thermal light,” *Journal of Modern Optics* **56**, 422 (2009).
- [11] X.-H. Chen *et al.*, “High-visibility, high-order lensless ghost imaging with thermal light,” *Opt. Lett.* **35**, 1166 (2010).
- [12] P.-A. Moreau *et al.*, “Ghost Imaging Using Optical Correlations,” *Laser Photonics Rev.* p. 1700143 (2017).
- [13] D.-Z. Cao, G.-J. Ge, and K. Wang, “Two-photon subwavelength lithography with thermal light,” *Applied Physics Letters* **97**, 051105 (2010).
- [14] G. Lu *et al.*, “Improving Visibility of Diffraction Pattern with Pseudo-Thermal Light,” *Chinese Physics Letters* **25**, 1277 (2008).
- [15] J. Sprigg, T. Peng, and Y. Shih, “Super-resolution imaging using the spatial-frequency filtered intensity fluctuation correlation,” *Sci. Rep.* (2016).
- [16] H. Lajunen *et al.*, “Resolution-enhanced optical coherence tomography based on classical intensity interferometry,” *J. Opt. Soc. Am. A* **26**, 1049 (2009).
- [17] C. López-Mariscal and J. C. Gutiérrez-Vega, “Observation of optical guiding using thermal light,” *Journal of Optics* **12**, 075702 (2010).
- [18] D. J. Ulness, “On the Role of Classical Field Time Correlations in Noisy Light Spectroscopy: Color Locking and a Spectral Filter Analogy,” *J. Chem. Phys.* **107**, 8111 (2003).
- [19] D. B. Turner *et al.*, “Coherent multidimensional optical spectra measured using incoherent light,” *Nat Commun* **4** (2013).
- [20] G. Li *et al.*, “Correction of photon statistics of quantum states in single-photon detection,” in *Quantum Optics and Applications in Computing and Communications II*, **5631**, 134 (2005).
- [21] T. Iskhakov *et al.*, “Intensity correlations of thermal light,” *The European Physical Journal Special Topics* **199**, 127 (2011).
- [22] J. Zhu *et al.*, “Thermal-light-based ranging using second-order coherence,” *Applied optics* **51**, 4885 (2012).
- [23] A. Jechow *et al.*, “Enhanced two-photon excited fluorescence from imaging agents using true thermal light,” *Nature Photonics* **7**, 973 EP (2013).
- [24] S. Hartmann *et al.*, “Tailored quantum statistics from broadband states of light,” *New J. Phys.* **17**, 043039 (2015).
- [25] J. Mika *et al.*, “Broadband thermal light with Bose-Einstein photon statistics from warm atomic vapor,” arXiv:1801.10555 [quant-ph] (2018).
- [26] T. F. Schulz *et al.*, “Complete cancellation of noise by means of color-locking in nearly degenerate, four-wave mixing of noisy light,” *J. Opt. Soc. Am. B* **22**, 1052 (2005).
- [27] A. Christ *et al.*, “Probing multimode squeezing with correlation functions,” *New Journal of Physics* **13**, 033027 (2011).
- [28] K. Y. Spasibko *et al.*, “Multiphoton Effects Enhanced due to Ultrafast Photon-Number Fluctuations,” *Phys. Rev. Lett.* **119**, 223603 (2017).
- [29] Z. Vernon *et al.*, “Truly unentangled photon pairs without spectral filtering,” *Optics letters* **42**, 3638 (2017).
- [30] B. Blauensteiner *et al.*, “Photon bunching in parametric down-conversion with continuous-wave excitation,” *Phys. Rev. A* **79**, 063846 (2009).
- [31] A. Eckstein *et al.*, “Highly efficient single-pass source of pulsed single-mode twin beams of light,” *Physical Review Letters* **106**, 013603 (2011).
- [32] K. Y. Spasibko, T. S. Iskhakov, and M. V. Chekhova, “Spectral properties of high-gain parametric down-conversion,” *Opt. Express* **20**, 7507 (2012).
- [33] K. Wakui *et al.*, “Ultrabroadband direct detection of nonclassical photon statistics at telecom wavelength,” *Scientific Reports* **4**, 4535 EP (2014).
- [34] J. Huang and P. Kumar, “Photon-counting statistics of multimode squeezed light,” *Phys. Rev. A* **40**, 1670 (1989).
- [35] V. Ansari *et al.*, “Tomography and purification of the temporal-mode structure of quantum light,” *Physical review letters* **120**, 213601 (2018).
- [36] Y. Zhou *et al.*, “Superbunching pseudothermal light with intensity modulated laser light and rotating groundglass,” ArXiv e-prints (2018).
- [37] W. F. Stinespring, “Positive functions on C*-algebras,” *Proceedings of the American Mathematical Society* **6**, 211 (1955).
- [38] W. P. Grice and I. A. Walmsley, “Spectral information and distinguishability in type-II down-conversion with a broadband pump,” *Phys. Rev. A* **56**, 1627 (1997).
- [39] N. Quesada and J. E. Sipe, “Effects of time ordering in quantum nonlinear optics,” *Phys. Rev. A* **90**, 063840 (2014).
- [40] N. Quesada and J. E. Sipe, “Time-Ordering Effects in the Generation of Entangled Photons Using Nonlinear Optical Processes,” *Phys. Rev. Lett.* **114**,

- 093903 (2015).
- [41] N. Quesada and A. M. Brańczyk, “Gaussian functions are optimal for waveguided nonlinear-quantum-optical processes,” ArXiv e-prints (2018).
 - [42] N. Quesada and J. E. Sipe, *In preparation*.
 - [43] R. J. Glauber, “The Quantum Theory of Optical Coherence,” Phys. Rev. **130**, 2529 (1963).
 - [44] R. Loudon, *The Quantum Theory of Light* (Clarendon Press, Oxford, 1983).
 - [45] A. M. Weiner, “Ultrafast optical pulse shaping: A tutorial review,” Optics Communications **284**, 3669 (2011).
 - [46] A. M. Brańczyk *et al.*, “Engineered optical nonlinearity for quantum light sources,” Opt. Express **19**, 55 (2011).
 - [47] P. B. Dixon, J. H. Shapiro, and F. N. C. Wong, “Spectral engineering by Gaussian phase-matching for quantum photonics,” Opt. Express **21**, 5879 (2013).
 - [48] A. Dosseva, L. Cincio, and A. M. Brańczyk, “Shaping the joint spectrum of down-converted photons through optimized custom poling,” Phys. Rev. A **93**, 013801 (2016).
 - [49] J.-L. Tambasco *et al.*, “Domain engineering algorithm for practical and effective photon sources,” Opt. Express **24**, 19616 (2016).
 - [50] F. Graffitti *et al.*, “Pure down-conversion photons through sub-coherence-length domain engineering,” Quantum Science and Technology **2**, 035001 (2017).
 - [51] V. Ansari *et al.*, “Tailoring nonlinear processes for quantum optics with pulsed temporal-mode encodings,” Optica **5**, 534 (2018).
 - [52] O. Kuzucu *et al.*, “Joint temporal density measurements for two-photon state characterization,” Physical review letters **101**, 153602 (2008).
 - [53] F. Graffitti *et al.*, “Independent high-purity photons created in domain-engineered crystals,” Optica **5**, 514 (2018).
 - [54] N. Quesada and A. M. Brańczyk, “Gaussian functions are optimal for waveguided nonlinear-quantum-optical processes,” Phys. Rev. A **98**, 043813 (2018).
 - [55] A. M. Pérez *et al.*, “Giant narrowband twin-beam generation along the pump-energy propagation direction,” Nature communications **6**, 7707 (2015).
 - [56] K. Y. Spasibko *et al.*, “Ring-shaped spectra of parametric downconversion and entangled photons that never meet,” Optics letters **41**, 2827 (2016).
 - [57] X.-P. Jiang and P. Brumer, “Creation and dynamics of molecular states prepared with coherent vs partially coherent pulsed light,” The Journal of Chemical Physics **94**, 5833 (1991).
 - [58] T. Mančal and L. Valkunas, “Exciton dynamics in photosynthetic complexes: excitation by coherent and incoherent light,” New Journal of Physics **12**, 065044 (2010).
 - [59] K. Hoki and P. Brumer, “Excitation of Biomolecules by Coherent vs. Incoherent Light: Model Rhodopsin Photoisomerization,” Procedia Chemistry **3**, 122 (2011).
 - [60] P. Brumer and M. Shapiro, “Molecular response in one-photon absorption via natural thermal light vs. pulsed laser excitation,” Proceedings of the National Academy of Sciences **109**, 19575 (2012).
 - [61] I. Kassal, J. Yuen-Zhou, and S. Rahimi-Keshari, “Does Coherence Enhance Transport in Photosynthesis?,” The Journal of Physical Chemistry Letters **4**, 362 (2013).
 - [62] A. Chenu *et al.*, “Thermal Light Cannot Be Represented as a Statistical Mixture of Single Pulses,” Phys. Rev. Lett. **114**, 213601 (2015).
 - [63] A. Chenu, A. M. Brańczyk, and J. E. Sipe, “First-order decomposition of thermal light in terms of a statistical mixture of single pulses,” Phys. Rev. A **91**, 063813 (2015).
 - [64] A. M. Brańczyk, A. Chenu, and J. E. Sipe, “Thermal light as a mixture of sets of pulses: the quasi-1D example,” J. Opt. Soc. Am. B **34**, 1536 (2017).
 - [65] I. B. Bobrov *et al.*, “Schmidt-like coherent mode decomposition and spatial intensity correlations of thermal light,” New Journal of Physics **15**, 073016 (2013).

Appendix A: Derivation of $G^{(1)}(\omega, \omega')$ and $G^{(2)}(\omega, \omega')$

In this section, we derive the frequency second- and fourth-order moments of the a fields. For the second-order moment, we use the relations in Eq. (5) to write

$$\langle \hat{a}^\dagger(\omega) \hat{a}(\omega') \rangle_\psi = \sum_{kl} \phi_k^*(\omega) \phi_l(\omega) \langle A_k^\dagger A_l \rangle_\psi. \quad (\text{A1})$$

We then use the linear Bogoliubov transformations in Eqs. (9) to write

$$\langle A_k^\dagger A_l \rangle_\psi = \langle \text{vac} | \hat{\mathcal{U}}_{\text{SQ}}^\dagger \hat{A}_k \hat{\mathcal{U}}_{\text{SQ}} \hat{\mathcal{U}}_{\text{SQ}}^\dagger \hat{A}_l \hat{\mathcal{U}}_{\text{SQ}} | \text{vac} \rangle \quad (\text{A2})$$

$$= \langle \text{vac} | \left(\cosh(r_k) \hat{A}_k + \sinh(r_k) \hat{B}_k^\dagger \right) \left(\cosh(r_l) \hat{A}_l + \sinh(r_l) \hat{B}_l^\dagger \right) | \text{vac} \rangle \quad (\text{A3})$$

$$= \sinh(r_k) \sinh(r_l) \langle \text{vac} | \hat{B}_k \hat{B}_l^\dagger | \text{vac} \rangle \quad (\text{A4})$$

$$= \sinh^2(r_k) \delta_{k,l} . \quad (\text{A5})$$

Plugging this result into Eq. (A1), we obtain

$$\langle \hat{a}^\dagger(\omega) \hat{a}(\omega') \rangle_\psi = \sum_k \sinh^2(r_k) \phi_k^*(\omega) \phi_k(\omega') . \quad (\text{A6})$$

Now let us consider the fourth-order moment

$$\langle \hat{a}^\dagger(\omega) \hat{a}^\dagger(\omega') \hat{a}(\omega) \hat{a}(\omega') \rangle_\psi = \sum_{k,l,m,n} \phi_k(\omega) \phi_l(\omega') \phi_m^*(\omega) \phi_n^*(\omega') \langle \hat{A}_k^\dagger \hat{A}_l^\dagger \hat{A}_m \hat{A}_n \rangle_\psi , \quad (\text{A7})$$

As before we look at the expectation value

$$\langle \hat{A}_k^\dagger \hat{A}_l^\dagger \hat{A}_m \hat{A}_n \rangle_\psi = \langle \text{vac} | \hat{\mathcal{U}}_{\text{SQ}}^\dagger \hat{A}_k^\dagger \hat{\mathcal{U}}_{\text{SQ}} \hat{\mathcal{U}}_{\text{SQ}}^\dagger \hat{A}_l^\dagger \hat{\mathcal{U}}_{\text{SQ}} \hat{\mathcal{U}}_{\text{SQ}}^\dagger \hat{A}_m \hat{\mathcal{U}}_{\text{SQ}} \hat{\mathcal{U}}_{\text{SQ}}^\dagger \hat{A}_n \hat{\mathcal{U}}_{\text{SQ}} | \text{vac} \rangle , \quad (\text{A8})$$

and use the linear Bogoliubov transformation then expand to obtain

$$\langle \hat{A}_k^\dagger \hat{A}_l^\dagger \hat{A}_m \hat{A}_n \rangle_\psi = \sinh(r_k) \sinh(r_l) \sinh(r_m) \sinh(r_n) \langle \text{vac} | \hat{B}_k \hat{B}_l \hat{B}_m^\dagger \hat{B}_n^\dagger | \text{vac} \rangle \quad (\text{A9})$$

$$= \sinh^2(r_k) \sinh^2(r_l) \delta_{k,m} \delta_{l,n} + \sinh^2(r_k) \sinh^2(r_l) \delta_{k,n} \delta_{l,m} . \quad (\text{A10})$$

Plugging these results into Eq. (A7), we find

$$\langle \hat{a}^\dagger(\omega) \hat{a}^\dagger(\omega') \hat{a}(\omega) \hat{a}(\omega') \rangle_\psi = \langle \hat{a}^\dagger(\omega) \hat{a}(\omega) \rangle_\psi \langle \hat{a}^\dagger(\omega') \hat{a}(\omega') \rangle_\psi + \langle \hat{a}^\dagger(\omega) \hat{a}(\omega') \rangle_\psi \langle \hat{a}^\dagger(\omega') \hat{a}(\omega) \rangle_\psi , \quad (\text{A11})$$

where the terms are give by Eq. (A6).

Appendix B: Derivation of $G^{(1)}(t, t')$ and $G^{(2)}(t, t')$

The first-order temporal correlation function for mode a is given by [43]

$$G_a^{(1)}(t_1, t_2) = \langle \hat{E}_a^{(-)}(t_1) \hat{E}_a^{(+)}(t_2) \rangle_\psi , \quad (\text{B1})$$

where $\hat{E}_a^{(\pm)}(t_1)$ are the usual positive/negative frequency components of the electric field operator in mode a . To simplify calculations, we follow Christ *et al.* [27] and replace the electric field operators by photon number creation and destruction operators ($\hat{E}_a^{(+)} \propto \hat{a}(t)$). This is valid when the spectra of the beams are not too spectrally broad. We thus have

$$G_a^{(1)}(t_1, t_2) = \langle \hat{a}^\dagger(t_1) \hat{a}(t_2) \rho_a \rangle_\psi . \quad (\text{B2})$$

We now use the relationship

$$\hat{a}(t) = \frac{1}{\sqrt{2\pi}} \int d\omega \hat{a}(\omega) e^{i\omega t} = \frac{1}{\sqrt{2\pi}} \int d\omega \left(\sum_k \phi_k^*(\omega) \hat{A}_k \right) e^{i\omega t} \equiv \sum_k \hat{A}_k \tilde{\phi}_k^*(t) , \quad (\text{B3})$$

where $\tilde{\phi}_k(t) = \frac{1}{\sqrt{2\pi}} \int d\omega \phi_k(\omega) e^{-i\omega t}$. This gives

$$G_a^{(1)}(t_1, t_2) = \left\langle \left(\sum_k \hat{A}_k^\dagger \tilde{\phi}_k(t_1) \right) \left(\sum_l \hat{A}_l \tilde{\phi}_l^*(t_2) \right) \right\rangle_\psi \quad (\text{B4})$$

$$= \sum_{k,l} \tilde{\phi}_k(t_1) \tilde{\phi}_l^*(t_2) \left\langle \hat{A}_k^\dagger \hat{A}_l \right\rangle_\psi. \quad (\text{B5})$$

Using the result in Eq. (A5), we have

$$G_a^{(1)}(t_1, t_2) = \sum_{k,l} \tilde{\phi}_k(t_1) \tilde{\phi}_l^*(t_2) \sinh^2(r_k) \delta_{k,l} \quad (\text{B6})$$

$$= \sum_k \tilde{\phi}_k(t_1) \tilde{\phi}_k^*(t_2) \sinh^2(r_k) \quad (\text{B7})$$

$$= \sum_k \tilde{\phi}_k(t_1) \tilde{\phi}_k^*(t_2) \bar{n}_k, \quad (\text{B8})$$

where \bar{n}_k is defined in Eq. (14).

The second-order temporal correlation function for mode a is given by [43]

$$G_a^{(2)}(t_1, t_2) = \langle \hat{a}^\dagger(t_1) \hat{a}^\dagger(t_2) \hat{a}(t_1) \hat{a}(t_2) \rangle_\psi. \quad (\text{B9})$$

Using a similar procedure as above, we can write this as

$$G_a^{(2)}(t_1, t_2) = \sum_{k,l,m,n} \tilde{\phi}_k(t_1) \tilde{\phi}_l(t_2) \tilde{\phi}_m^*(t_1) \tilde{\phi}_n^*(t_2) \left\langle \hat{A}_k^\dagger \hat{A}_l^\dagger \hat{A}_m \hat{A}_n \right\rangle_\psi. \quad (\text{B10})$$

Using Eq. (A10), we have

$$G_a^{(2)}(t_1, t_2) = \sum_{k,l,m,n} \tilde{\phi}_k(t_1) \tilde{\phi}_l(t_2) \tilde{\phi}_m^*(t_1) \tilde{\phi}_n^*(t_2) \quad (\text{B11})$$

$$\times (\sinh^2(r_k) \sinh^2(r_l) \delta_{k,m} \delta_{l,n} + \sinh^2(r_k) \sinh^2(r_l) \delta_{k,n} \delta_{l,m})$$

$$= \sum_k \tilde{\phi}_k(t_1) \tilde{\phi}_k^*(t_1) \bar{n}_k \sum_l \tilde{\phi}_l(t_2) \tilde{\phi}_l^*(t_2) \bar{n}_l + \sum_k \tilde{\phi}_k(t_1) \tilde{\phi}_k^*(t_2) \bar{n}_k \sum_l \tilde{\phi}_l(t_2) \tilde{\phi}_l^*(t_1) \bar{n}_l, \quad (\text{B12})$$

where \bar{n}_k is defined in Eq. (14). Comparing with the result in Eq. (B8), we find that

$$G_a^{(2)}(t_1, t_2) = G_a^{(1)}(t_1, t_1) G_a^{(1)}(t_2, t_2) + G_a^{(1)}(t_1, t_2) G_a^{(1)}(t_2, t_1). \quad (\text{B13})$$